PHILOSOPHICAL TRANSACTIONS A

royalsocietypublishing.org/journal/rsta

Research

Cite this article: Bashkirtseva I, Slepukhina E. 2022 Variability of complex oscillatory regimes in the stochastic model of cold-flame combustion of a hydrocarbon mixture. *Phil. Trans. R. Soc. A* **380**: 20200314.
https://doi.org/10.1098/rsta.2020.0314

Received: 12 January 2021
Accepted: 4 February 2021

One contribution of 15 to a theme issue 'Transport phenomena in complex systems (part 2)'.

Subject Areas:
mathematical modelling, physical chemistry, differential equations, statistics

Keywords:
combustion model, gas mixture, bistability, stochastic transport, noise-induced oscillations

Author for correspondence:
E. Slepukhina
e-mail:
Evdokiia.Slepukhina@uni-hohenheim.de

Variability of complex oscillatory regimes in the stochastic model of cold-flame combustion of a hydrocarbon mixture

I. Bashkirtseva[1] and E. Slepukhina[2]

[1]Ural Federal University, Ekaterinburg, Russia
[2]University of Hohenheim, Stuttgart, Germany

ES, 0000-0003-3523-6147

Processes of the cold-flame combustion of a mixture of two hydrocarbons are studied on the base of a three-dimensional nonlinear dynamical model. Bifurcation analysis of the deterministic model reveals mono- and bistability parameter zones with equilibrium and oscillatory attractors. For this model, effects of random disturbances in the bistability parameter zone are studied. We show that random forcing causes transitions between coexisting stable equilibria and limit cycles with the formation of complex stochastic mixed-mode oscillations. Properties of these oscillatory regimes are studied by means of statistics of interspike intervals. A phenomenon of anti-coherence resonance is discussed.

This article is part of the theme issue 'Transport phenomena in complex systems (part 2)'.

1. Introduction

The study of complex combustion modes is a fundamental problem of thermochemistry [1,2]. An important step in understanding the general mechanisms of complex combustion processes was the transition to the study of mathematical models that allows us to describe the processes of chemical thermokinetics using differential equations. The foundations of mathematical modelling and analysis of thermokinetics were laid out in the works of Semenov [3], Zeldovich [4], Frank-Kamenetsky [5], Amundson [6], Aris [7,8], and their followers (see [9,10] and references therein).

THE ROYAL SOCIETY PUBLISHING

royalsocietypublishing.org/journal/rsta Phil. Trans. R. Soc. A 380: 20200314

A wide range of two-dimensional dynamic models are now known that describe the kinetics of these reactions in terms of reactant concentration and reactor temperature [11–16]. From a mathematical point of view, the diversity of kinetic regimes is connected with the appearance of self-oscillatory regimes and multistability with the coexistence of several attractors of different types. A study of these kinetic regimes is based on the theory of bifurcations and analysis of basins of attraction. It is well known that in dynamical models with strong nonlinearity even seemingly small random disturbances can complicate behaviour and cause stochastic transport [17–19] with various unexpected noise-induced effects [20–29]. Here, the phenomena of coherence and anti-coherence resonance attract attention of researchers [30–36].

Stochastic disturbances in nonlinear models of thermochemical processes can generate abrupt changes in temperature and concentration with the appearance of complex oscillatory regimes [37–41]. At present, mathematical modelling of the combustion processes of mixtures of reagents is a challenging problem of modern thermochemistry [10,42–45]. To simulate the combustion process of a mixture of two reagents, systems of three differential equations are used, in which, as is known, not only periodic but also quasi-periodic and chaotic oscillations are possible.

A significant number of investigations are devoted to the study of the dynamic processes of combustion of hydrocarbon mixtures. In the present paper, we investigate a three-dimensional model of the cold-flame combustion of a mixture of two hydrocarbons. This simple conceptual model was proposed in [46] to describe the self-oscillation regime of the cool-flame combustion of an *n*-heptane-isooctane mixture. Numerical simulations based on this model have shown good qualitative agreement with experimental data [47]. A parametric analysis of this deterministic model is presented in [10]. The present paper aims to study how noise affects the system and generates complex oscillatory modes.

In §2, the deterministic features of the model are described. In §3, we study effects of random disturbances on the model in the parameter region where the initial deterministic system is bistable. We show that under noise, transitions between coexisting stable equilibria and limit cycles arise that form stochastic mixed-mode oscillations. Properties of these complex oscillatory regimes are studied by means of statistics of interspike intervals.

2. Deterministic model

Consider the three-dimensional model of the cold-flame combustion of a mixture of two hydrocarbons [46]

$$\left.\begin{aligned} \dot{x}_1 &= f_1(y)\,(1-x_1) - x_1 \\ \dot{x}_2 &= f_2(y)\,(1-x_2) - x_2 \\ \text{and}\qquad \dot{y} &= \beta_1 f_1(y)(1-x_1) + \beta_2 f_2(y)(1-x_2) + (1-y) - s(y-\bar{y}), \end{aligned}\right\} \tag{2.1}$$

where

$$f_i(y) = Da_i\ \exp\left[\gamma_i\left(1-\frac{1}{y}\right)\right], \quad i=1,2.$$

Here, the variables x_1 and x_2 correspond to the concentrations of two reagents (*n*-heptane and isooctane), and y is the temperature. Da_i, β_i, γ_i, s, $\bar{y}$ are dimensionless parameters of the model. In this paper, following [10], we fix

$$Da_1 = 0.14,\ \ Da_2 = 0.001,\ \ \beta_1 = 0.25,\ \ \beta_2 = 0.5,\ \ s = 2,\ \ \bar{y} = 1,\ \ \gamma_2 = 40,$$

and study the dynamics of the system varying the parameter γ_1.

Figure 1 shows the bifurcation diagram of the model (2.1). The system has one equilibrium point, which is stable in the regions $\gamma_1 < B_2 \approx 47.71$ and $\gamma_1 > B_3 \approx 55.29$. The equilibrium switches its stability due to two Andronov–Hopf (AH) bifurcations: via the subcritical AH bifurcation at the point $\gamma_1 = B_2$ an unstable limit cycle arises, and at the point $\gamma_1 = B_3$ due to the supercritical AH

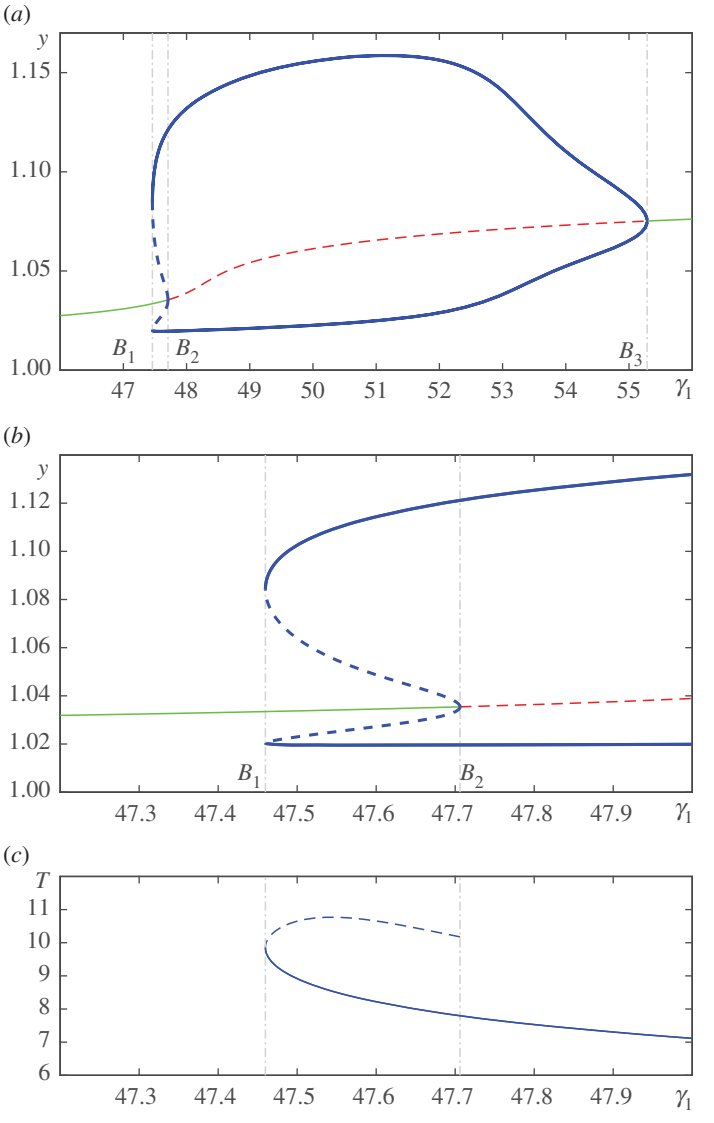

Figure 1. Bifurcation diagram of system (2.1) in dependence on the parameter γ_1: (*a*) *y*-coordinates of stable (green solid) and unstable (red dashed) equilibria, minimal and maximal values of *y*-coordinate along stable (blue solid) and unstable (blue dashed) limit cycles; (*b*) zoom into the zone of bistability; (*c*) period of limit cycles. B_1 ($\gamma_1 \approx 47.46$) is the point of the saddle-node bifurcation of limit cycles, B_2 ($\gamma_1 \approx 47.71$) is the subcritical Andronov–Hopf bifurcation point, B_3 ($\gamma_1 \approx 55.29$) is the supercritical Andronov–Hopf bifurcation point. (Online version in colour.)

bifurcation a stable limit cycle is born. The stable and unstable limit cycles coincide and disappear at the point $\gamma_1 = B_1 \approx 47.46$ due to the saddle-node bifurcation of the limit cycles.

Thus, the system (2.1) has three qualitatively different types of behaviour. For $\gamma_1 < B_1$ and $\gamma_1 > B_3$, the system is monostable, and the only attractor is the stable equilibrium. In the parameter zone $\gamma_1 \in (B_1, B_2)$, the dynamic regime is bistable: the stable equilibrium coexists with the stable limit cycle, and phase trajectories tend to one or another attractor depending on initial conditions. For $\gamma_1 \in (B_2, B_3)$, the system is monostable, and the attractor is the stable limit cycle. Figure 2 displays three typical phase portraits of the deterministic system (2.1) for $\gamma_1 = 47.4$ (monostability with the stable equilibrium), $\gamma_1 = 47.5$ (bistability), and $\gamma_1 = 47.8$ (monostability with the stable limit cycle).

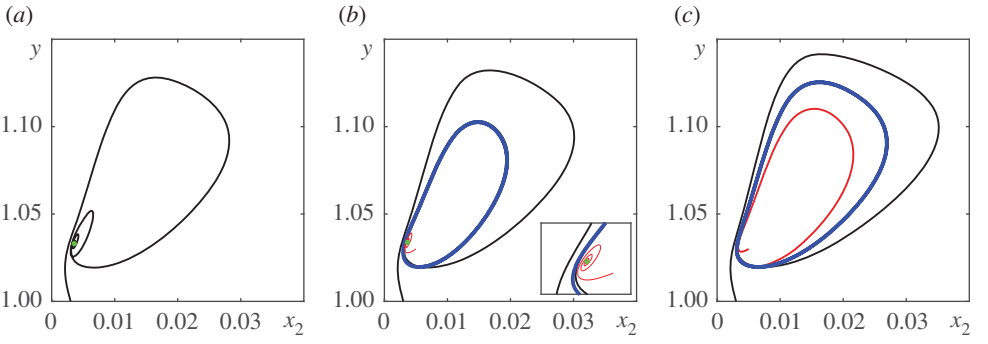

Figure 2. Phase portraits of the deterministic system (2.1) (in projection on the $x_2 - y$-plane): (*a*) $\gamma_1 = 47.4$ (stable equilibrium); (*b*) $\gamma_1 = 47.5$ (coexistence of stable equilibrium and limit cycle); (*c*) $\gamma_1 = 47.8$ (stable limit cycle). Blue lines show stable limit cycles, green circles mark positions of stable equilibria, black and red lines show phase trajectories. (Online version in colour.)

These features of the deterministic model play an important role in understanding the stochastic phenomena that arise when the system is exposed to random disturbances.

3. Variability of complex oscillatory regimes in stochastic model

Let us study the influence of random disturbances on the system (2.1). For this purpose consider the stochastic model

$$\left.\begin{aligned} \dot{x}_1 &= f_1(y)(1-x_1) - x_1 \\ \dot{x}_2 &= f_2(y)(1-x_2) - x_2 \\ \text{and} \quad \dot{y} &= \beta_1 f_1(y)(1-x_1) + \beta_2 f_2(y)(1-x_2) + (1-y) - s(y-\bar{y}) + \varepsilon\xi(t), \end{aligned}\right\} \tag{3.1}$$

where the random component is described by the standard white Gaussian noise $\xi(t)$ with probabilistic properties $\langle \xi(t) \rangle = 0$, $\langle \xi(t)\xi(t+\tau) \rangle = \delta(\tau)$ and the intensity ε.

In this paper, we focus on the noise effects in the bistability zone $\gamma_1 \in (B_1, B_2)$ of the parameter space, where in the deterministic system (2.1), the stable limit cycle and the stable equilibrium coexist.

Consider first the value $\gamma_1 = 47.5$. Figure 4 shows random trajectories of the system (3.1) that start from the deterministic limit cycle and the corresponding time series $y(t)$. For a relatively small noise intensity $\varepsilon = 0.0001$ (figure 4*a*), the trajectories locate near the limit cycle, and the system has a large amplitude oscillatory mode. For a greater noise $\varepsilon = 0.0002$ (figure 4*b*), one can observe that the trajectories leave the limit cycle and approach the equilibrium, so that the large amplitude oscillations switch to the small amplitude ones. Thus, for this level of random disturbances, a noise-induced transition from the basin of attraction of the limit cycle to the basin of attraction of the equilibrium arises. With a further increase of the noise intensity (see figure 4*c* for $\varepsilon = 0.0005$), backward transitions from the basin of attraction of the equilibrium to the one of the limit cycle appear so that the stochastic system shows mixed-mode oscillations.

Consider also the parameter value $\gamma_1 = 47.6$ and stochastic trajectories starting from the stable equilibrium (figure 3). For a small noise level $\varepsilon = 0.0001$ (figure 3*a*), one can observe small-amplitude oscillations near the equilibrium. With an enhancement of the noise intensity (see figure 3*b* for $\varepsilon = 0.0003$), the stochastic trajectories leave the basin of attraction of the equilibrium and move to the basin of attraction of the limit cycle, wherein the small-amplitude oscillations switch to large-amplitude ones. For the greater noise level $\varepsilon = 0.0005$ (figure 3*c*), the backward transitions to the basin of attraction of the limit cycle are observed. Such mutual transitions between the attractors form the mixed-mode oscillations.

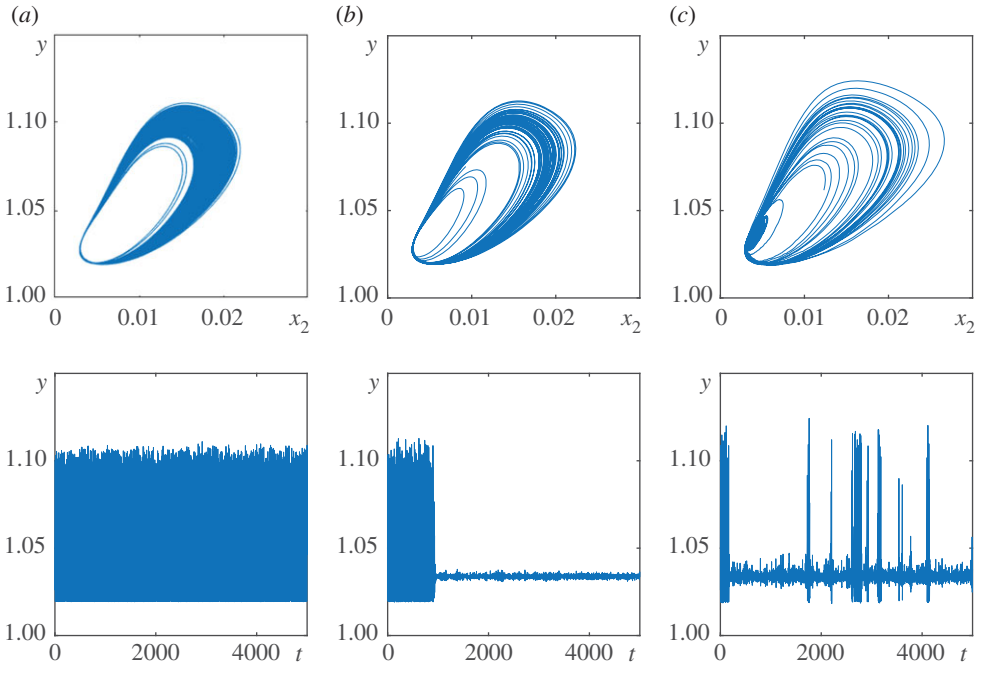

Figure 3. Projections of system (3.1) stochastic trajectories on the $x_2 - y$-plane (above) and corresponding time series $y(t)$ (below) starting from the stable equilibrium for $\gamma_1 = 47.6$: (*a*) $\varepsilon = 0.0001$, (*b*) $\varepsilon = 0.0003$ (*c*) $\varepsilon = 0.0005$. (Online version in colour.)

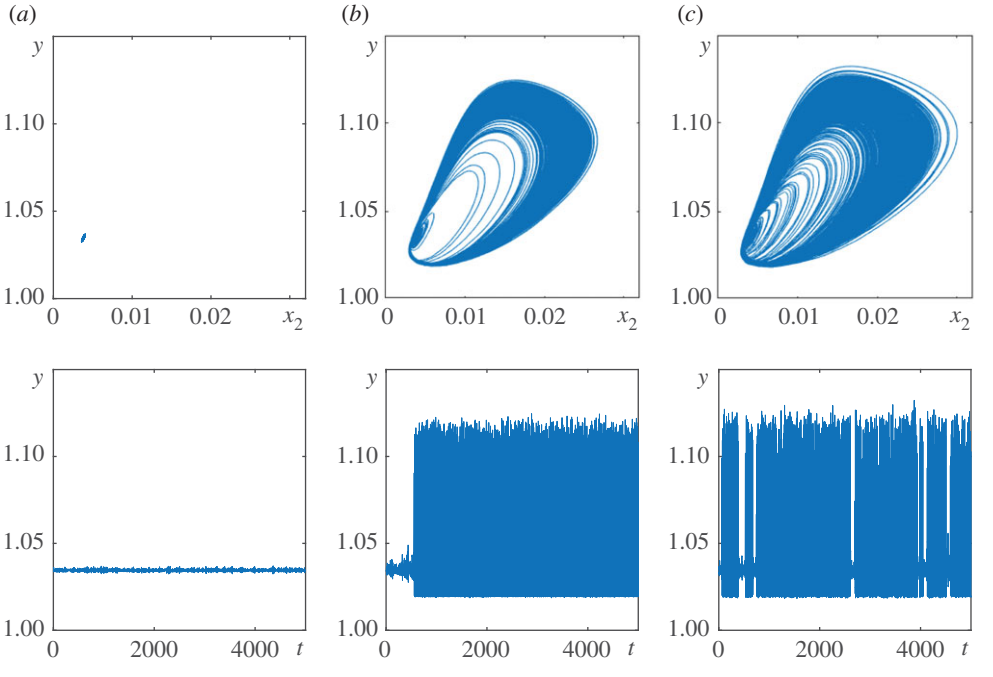

Figure 4. Projections of system (3.1) stochastic trajectories on the $x_2 - y$-plane (above) and corresponding time series $y(t)$ (below) starting from the stable limit cycle for $\gamma_1 = 47.5$: (*a*) $\varepsilon = 0.0001$, (*b*) $\varepsilon = 0.0002$ and (*c*) $\varepsilon = 0.0005$. (Online version in colour.)

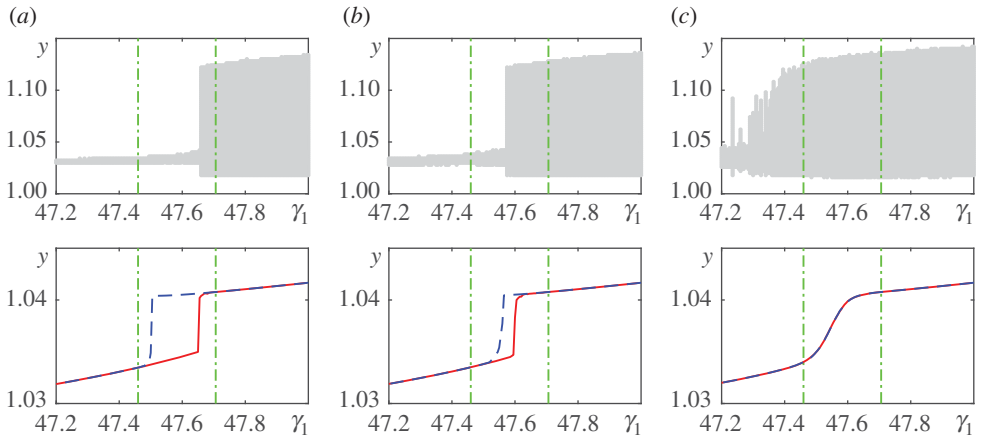

Figure 5. Random states (above) of the system (3.1) solutions starting from the stable equilibrium and average values (below) of the system solutions starting from the stable equilibrium (red solid) and stable limit cycle (blue dashed) in dependence on the parameter γ_1: (*a*) $\varepsilon = 0.0001$, (*b*) $\varepsilon = 0.0002$, (*c*) $\varepsilon = 0.0005$. Green dash-dotted lines show the borders of the bistability zone (B_1, B_2) of the deterministic system. (Online version in colour.)

These noise-induced changes in the dynamics are reflected in the plots of random states of the system solutions in dependence on the parameter γ_1. Figure 5 (above) displays such plots for the stochastic trajectories that start from the equilibria for three values of the noise intensity: $\varepsilon = 0.0001$, $\varepsilon = 0.0002$ and $\varepsilon = 0.0005$. One can see that under noise, the parameter region of large amplitude oscillations expands so that such oscillations are observed for smaller values of γ_1. Noise-induced transitions to the basin of attraction of the limit cycle appear in the zone of bistability, and moreover, for $\varepsilon = 0.0005$, a stochastic generation of large-amplitude oscillations arises even in the region where the deterministic system is monostable in an equilibrium regime.

When system solutions start from the limit cycle, noise-induced transitions to the basin of attraction of the equilibrium also appear. Details of mutual transitions between the coexisting attractors are displayed in figure 5 (below), where the average values of the system solutions starting from one or another attractor versus γ_1 are plotted for the same values of noise as in figure 5 (above). These plots show that with an increase of the noise intensity, the region of bistability becomes narrower. For sufficiently large values of ε (figure 5*c*), the lines of average values of solutions, starting from different attractors, coincide, i.e. the system becomes indifferent to the choice of initial values in the formation of stochastic mixed-mode oscillations.

Let us study this stochastic phenomenon in more detail. Consider statistical properties of temporal characteristics of oscillations, namely the mean values and the coefficients of variations of interspike intervals. Here, by an interspike interval we imply the time between two sequential large-amplitude excursions (spikes) away from the equilibrium. Figure 6 shows the mean values m and the coefficients of variation C_V of interspike intervals of stochastic trajectories starting from different attractors for $\gamma_1 = 47.5$ and $\gamma_1 = 47.6$ in dependence on the noise intensity.

When a trajectory starts from the stable equilibrium, for small values of noise intensity, the mean values of interspike intervals are close to infinity, because there are no large-amplitude oscillations. With an enhanced noise level, the values of m abruptly decrease which indicates a beginning of noise-induced transitions to the basin of attraction of the limit cycle. For trajectories starting from the limit cycle, for a small noise, the mean values m correspond to the period of the cycle. With an enhancement of the noise intensity, the values of m increase, which means that interspike intervals become longer due to the transitions to the basin of attraction of the equilibrium. The peak in values of $m(\varepsilon)$ is most distinctly visible for the value $\gamma_1 = 47.5$ (see figure 6*a*, above). As the noise intensity increases further, plots of $m(\varepsilon)$ for trajectories, starting from different attractors, coincide, which indicated mutual transitions between the coexisting

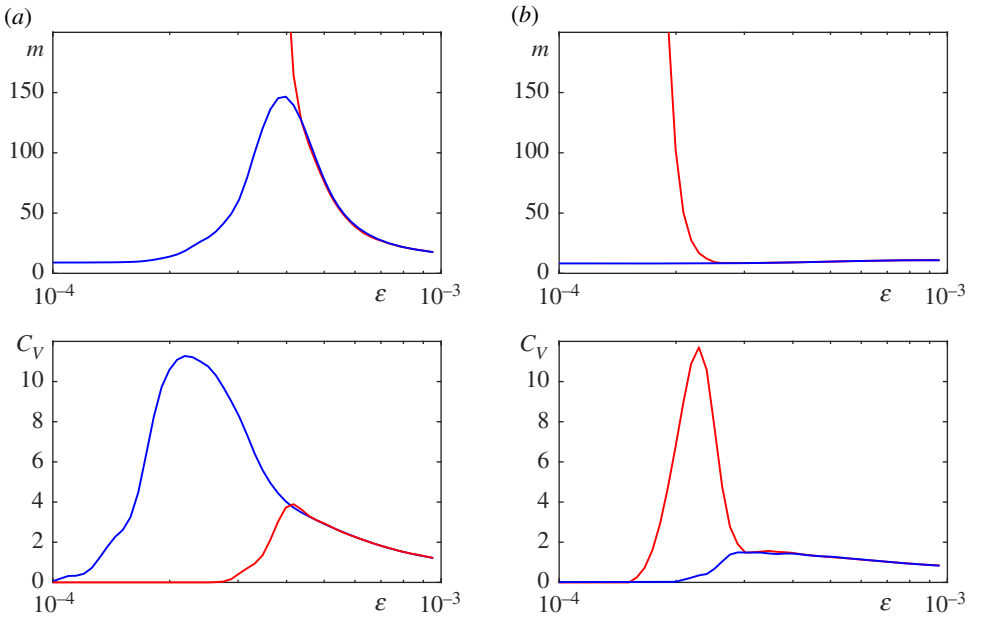

Figure 6. Mean values of m and coefficients of variation C_V of interspike intervals of system (3.1) trajectories starting from the stable equilibrium (red) and stable limit cycle (blue) for (*a*) $\gamma_1 = 47.5$ and (*b*) $\gamma_1 = 47.6$, depending on the noise intensity ε. (Online version in colour.)

attractors. Thus, for sufficiently large levels of noise, a phenomenon of noise-induced mixing occurs in the system.

The plots of the coefficients of variations (see figure 6, below) show peaks that correspond to the values of noise intensity with the largest variability in interspike intervals. This indicates a phenomenon of anti-coherence resonance. It occurs when noise-induced transitions to the other basin of attraction begin to appear, and the system is the most incoherent: the stochastic oscillations have interspike intervals of different length (short if trajectories are in the vicinity of the limit cycle, and very long if trajectories are located near the equilibrium). For greater noise intensities, the values of $C_V(\varepsilon)$ decrease, which indicates that the stochastic oscillations become more coherent. The lines of $C_V(\varepsilon)$, corresponding to different attractors, coincide, which indicates mutual noise-induced transitions and mixing.

4. Conclusion

This paper is devoted to the study of the causes of the emergence of complex oscillatory modes in combustion processes. This issue was investigated using the three-dimensional model describing the combustion process of a mixture of two hydrocarbons. By bifurcation analysis, we found parametric zones corresponding to various dynamic modes of mono- and bistable behaviour associated with equilibrium and self-oscillatory attractors. It was shown how the inevitably present random disturbances increase the variety of dynamical behaviour, giving rise to complex mixed-mode oscillations. The paper investigated stochastic excitability and noise-induced transitions between attractors. With the help of statistics of interspike intervals, we demonstrated the phenomenon of anti-coherence resonance and localized a parametric zone with high oscillatory variability.

Data accessibility. This article has no additional data.

Competing interests. We declare we have no competing interests.

Authors' contributions. All authors contributed equally to the present research article.

Funding. The work on bifurcation analysis was supported by the Ministry of Science and Higher Education of the Russian Federation (Ural Mathematical Center project no. 075-02-2020-1537/1). The work on the study of noise-induced effects was supported by RFBR (20-01-00165).

References

1. Spalding DB. 1979 *Combustion and mass transfer*. Oxford, UK: Pergamon.
2. Williams FA. 2018 *Combustion theory*. Boca Raton, FL: CRC Press.
3. Semenov NN. 1928 Theories of combustion processes. *Z. Phys. Chem.* **48**, 571–582.
4. Zeldovich JB, Zysin JA. 1941 On the theory of heat stress. Exothermic reaction in the jet. *Zh. Tekh. Fiz.* **11**, 501–508. (in Russian).
5. Frank-Kamenetskii DA. 1955 *Diffusion and heat exchange in chemical kinetics*. Princeton, NJ: Princeton University Press.
6. Aris R, Amundson N. 1958 An analysis of chemical reactor stability and control. *Chem. Eng. Sci.* **7**, 121–155. (doi:10.1016/0009-2509(58)80019-6)
7. Aris R. 1965 *Introduction to the analysis of chemical reactors*. Englewood Cliffs, NJ: Prentice-Hall.
8. Aris R. 1999 *Mathematical modeling: a chemical engineer's perspective*. New York, NY: Academic Press.
9. Ramkrishna D, Amundson NR. 2004 Mathematics in chemical engineering: a 50 year introspection. *AlChE J.* **50**, 7–23. (doi:10.1002/(ISSN)1547-5905)
10. Bykov VI, Tsybenova SB, Yablonsky G. 2018 *Chemical complexity via simple models*. Berlin, Germany: De Gruyter.
11. Volter BV, Salnikov IY. 1965 *Modeling and optimization of catalytic processes*. Moscow: Nauka. (in Russian).
12. Uppal A, Ray WH, Poore AB. 1974 On the dynamic behavior of continuous stirred tank reactors. *Chem. Eng. Sci.* **29**, 967–985. (doi:10.1016/0009-2509(74)80089-8)
13. Uppal A, Ray WH, Poore AB. 1976 The classification of the dynamic behavior of continuous stirred tank reactors—influence of reactor resident time. *Chem. Eng. Sci.* **31**, 205–214. (doi:10.1016/0009-2509(76)85058-0)
14. Bykov VI, Tsybenova SB, Slin'ko MG. 2001 Andronov–Hopf bifurcations in the Aris–Amundson model. *Dokl. Phys. Chem.* **378**, 134–137. (doi:10.1023/A:1019251012744)
15. Bykov VI, Tsybenova SB. 2001 Parametric analysis of the simplest model of the theory of thermal explosion—the Zel'dovich–Semenov model. *Combust. Explos. Shock Waves* **37**, 523–534. (doi:10.1023/A:1012384818482)
16. Kawczyński AL, Gorecki J. 1992 Molecular dynamics simulations of sustained oscillations in a thermochemical system. *J. Phys. Chem.* **96**, 1060–1067. (doi:10.1021/j100182a010)
17. Schadschneider A, Chowdhury D, Nishinari K. 2010 *Stochastic transport in complex systems: from molecules to vehicles*. Amsterdam, The Netherland: Elsevier.
18. Sahimi M, Hughes BD, Scriven LE, Davis HT. 1983 Stochastic transport in disordered systems. *J. Chem. Phys.* **782**, 6849–6864. (doi:10.1063/1.444631)
19. Guillet A, Roldan E, Julicher F. 2020 Extreme-value statistics of stochastic transport processes. *New J. Phys.* **22**, 123038. (doi:10.1088/1367-2630/abcf69)
20. Gao JB, Hwang SK, Liu JM. 1999 When can noise induce chaos? *Phys. Rev. Lett.* **82**, 1132–1135. (doi:10.1103/PhysRevLett.82.1132)
21. Lindner B, Garcia-Ojalvo J, Neiman A, Schimansky-Geier L. 2004 Effects of noise in excitable systems. *Phys. Rep.* **392**, 321–424. (doi:10.1016/j.physrep.2003.10.015)
22. Bashkirtseva G, Chen G, Ryashko L. 2010 Analysis of stochastic cycles in the Chen system. *Int. J. Bifurcation Chaos* **20**, 1439–1450. (doi:10.1142/S0218127410026587)
23. Anishchenko VS, Astakhov VV, Neiman AB, Vadivasova TE, Schimansky-Geier L. 2007 *Nonlinear dynamics of chaotic and stochastic systems. Tutorial and modern development*. Berlin, Heidelberg: Springer.
24. Ryashko L, Slepukhina E. 2017 Noise-induced torus bursting in the stochastic Hindmarsh-Rose neuron model. *Phys. Rev. E* **96**, 032212. (doi:10.1103/PhysRevE.96.032212)
25. Ryashko L. 2018 Sensitivity analysis of the noise-induced oscillatory multistability in Higgins model of glycolysis. *Chaos* **28**, 033602. (doi:10.1063/1.4989982)
26. Bashkirtseva I, Ryashko L. 2020 How additive noise forms and shifts phantom attractors in slow–fast systems. *J. Phys. A: Math. Theor.* **53**, 375008. (doi:10.1088/1751-8121/aba76f)

27. Kolinichenko AP, Pisarchik AN, Ryashko LB. 2020 Stochastic phenomena in pattern formation for distributed nonlinear systems. *Phil. Trans. R. Soc. A* **378**, 20190252. (doi:10.1098/rsta.2019.0252)
28. Kolinichenko A, Ryashko L. 2020 Multistability and stochastic phenomena in the distributed Brusselator model. *J. Comput. Nonlinear Dynam.* **15**, 011007. (doi:10.1115/1.4045405)
29. Ryashko L, Slepukhina E. 2020 Noise-induced toroidal excitability in neuron model. *Commun. Nonlinear Sci. Numer. Simul.* **82**, 105071. (doi:10.1016/j.cnsns.2019.105071)
30. Pikovsky AS, Kurths J. 1997 Coherence resonance in a noise-driven excitable system. *Phys. Rev. Lett.* **78**, 775–778. (doi:10.1103/PhysRevLett.78.775)
31. Pisarchik AN, Jaimes-Reátegui R. 2015 Deterministic coherence resonance in coupled chaotic oscillators with frequency mismatch. *Phys. Rev. E* **92**, 050901. (doi:10.1103/PhysRevE.92.050901)
32. García-Vellisca MA, Pisarchik AN, Jaimes-Reátegui R. 2016 Experimental evidence of deterministic coherence resonance in coupled chaotic systems with frequency mismatch. *Phys. Rev. E* **94**, 012218. (doi:10.1103/PhysRevE.94.012218)
33. Andreev AV, Makarov VV, Runnova AE, Pisarchik AN, Hramov AE. 2018 Coherence resonance in stimulated neuronal network. *Chaos Solitons Fractals* **106**, 80–85. (doi:10.1016/j.chaos.2017.11.017)
34. Pisarchik AN, Maksimenko VA, Andreev AV, Frolov NS, Makarov VV, Zhuravlev MO, Runnova AE, Hramov AE. 2019 Coherent resonance in the distributed cortical network during sensory information processing. *Sci. Rep.* **9**, 18325. (doi:10.1038/s41598-019-54577-1)
35. Bashkirtseva I, Ryashko L. 2020 Mixed-mode self-oscillations, stochastic excitability, and coherence resonance in flows of highly concentrated suspensions. *Nonlinear Dyn.* **102**, 1837–1848. (doi:10.1007/s11071-020-06025-3)
36. Zhu J. 2020 Phase sensitivity for coherence resonance oscillators. *Nonlinear Dyn.* **102**, 2281–2293. (doi:10.1007/s11071-020-06091-7)
37. van Kampen NG. 1987 *Stochastic processes in physics and chemistry*. Amsterdam, The Netherland: North-Holland.
38. Kawczyński AL, Nowakowski B. 2003 Master equation simulations of a model of a thermochemical system. *Phys. Rev. E* **68**, 036218. (doi:10.1103/PhysRevE.68.036218)
39. Kolbus A, Nowakowski B, Kawczyński AL. 2013 Distributions of first passage times in a bistable thermochemical system with a low temperature stationary state. *Eur. Phys. J. B* **86**, 262. (doi:10.1140/epjb/e2013-31146-9)
40. Bashkirtseva A, Fominykh PM. 2016 Analysis of the stochastic excitement in a model of flow reactor. *J. Siberian Fed. Univ. Math. Phys.* **9**, 269–278. (doi:10.17516/1997-1397-2016-9-3-269-278)
41. Bashkirtseva I. 2018 Controlling the stochastic sensitivity in thermochemical systems under incomplete information. *Kybernetika* **54**, 96–109.
42. Burger M, Field RJ. 1985 *Oscillations and traveling waves in chemical systems*. New York, NY: Wiley.
43. Slin'ko MM, Jaeger NI. 1994 *Oscillating heterogeneous catalytic systems*. Amsterdam, The Netherland: Elsevier.
44. Tihay V, Simeoni A, Santoni PA, Garo JP, Vantelon JP. 2009 A global model for the combustion of gas mixtures released from forest fuels. *Proc. Combust. Inst.* **32**, 2575–2582. (doi:10.1016/j.proci.2008.06.095)
45. Methling T, Braun-Unkhoff M, Riedel U. 2020 An optimised chemical kinetic model for the combustion of fuel mixtures of syngas and natural gas. *Fuel* **262**, 116611. (doi:10.1016/j.fuel.2019.116611)
46. Bykov VI, Kim VF, Yablonskii GS, Stepanskii YY. 1980 Modelling of self-oscillations in the combustion of *n*-heptane-isooctane mixtures. *React. Kinet. Catal. Lett.* **14**, 295–299. (doi:10.1007/BF02073494)
47. Stepanskii YY, Evmenenko NP, Yablonskii GS, Bykov VI. 1980 Self-oscillations in the cool-flame combustion of a model *n*-heptane-isooctane mixture. *React. Kinet. Catal. Lett.* **14**, 335–339. (doi:10.1007/BF02073501)